Temperature and bias-voltage dependent transport in magnetic tunnel junctions with low energy Ar-ion irradiated barriers

J. Schmalhorst* and G. Reiss
University of Bielefeld, Department of Physics, Nano Device Group, P.O. Box 100131, 33501 Bielefeld, Germany
(Received 29 April 2003; revised manuscript received 4 September 2003; published 31 December 2003)

Magnetic tunnel junctions ($Mn_{83}Ir_{17}/Co_{70}Fe_{30}/AlO_x/Ni_{80}Fe_{20}$) are investigated, whose barriers are irradiated by a low energy Ar^+ ion beam immediately after plasma oxidation of the aluminum film. The tunneling magnetoresistance prior to irradiation is up to 71% at 10 K. The ion irradiation increases the area resistance product up to a factor of 40 for ion energies up to 150 V. Further, the tunneling magnetoresistance and the dielectric stability is strongly reduced with increasing ion energies. From the analysis of the temperature and the voltage dependence of the tunneling magnetoresistance we conclude that this is due to an irradiation induced local change of the coordination of the Al and O atoms in the barrier. This leads to a thicker barrier and an increase of the precursor density for the dielectric breakdown. Further, an increase of hopping conductance through localized states is discussed. At energies larger than 150 V the resistance breaks down rapidly and the tunneling magnetoresistance vanishes completely. This results from the enhanced intermixing and sputtering of the barrier and electrode material. The results are also supported by investigations of the magnetic and the noise properties of the junctions and the Cu-K_α-reflectivity of AlO_x multilayers.

DOI: 10.1103/PhysRevB.68.224437 PACS number(s): 75.70.−i, 72.25.−b, 85.75.−d

I. INTRODUCTION

In recent years the interest in magnetic tunnel junctions (MTJ's) increased considerably, because MTJ's became a promising candidate for sensor and memory devices.[1] The formation of the tunnel barrier is the most challenging preparation step for MTJs.[2] The common preparation technique is a postoxidation of a thin aluminum film. Often, a mixture of Ar and O_2 is used for this plasma process. Thus the influence of a low energy Ar^+ bombardment on the properties is of large interest for the preparation of MTJ's. In this paper we discuss the transport properties of MTJ's whose barriers are irradiated by low energy Ar^+ ions immediately after plasma oxidation. In particular, the temperature and the voltage dependence of the tunneling magnetoresistance (TMR) is discussed with respect to different tunneling and transport mechanisms (direct and assisted tunneling, hopping conductance), which are the basis for the models proposed by Han *et al.*,[3] Dimopoulos,[4] and Shang *et al.*[5] The aim of these experiments is to understand the influence of the ion irradiation on the transport properties of the junctions. Particularly, the possibility of structural changes in the barrier is discussed. In general, we find a degradation of the properties of the MTJ's.

II. EXPERIMENT

The MTJs are prepared in a magnetron sputtering system with a base pressure of 1×10^{-7} mbar. The layer stack consists of $Cu^{30\ nm}/Ni_{80}Fe_{20}^{4\ nm}$ (Py1)/$Mn_{83}Ir_{17}^{15\ nm}/Co_{70}Fe_{30}^{3\ nm}/Al^{1.4\ nm}$ + oxidation + Ar^+ irradiation/$Ni_{80}Fe_{20}^{4\ nm}$ (Py2)/$Ta^{3\ nm}/Cu^{55\ nm}/Au^{20\ nm}$ on a thermally oxidized (100 nm) 4-inch silicon (100) wafer. The Al layer is oxidized for 100 s by a remote plasma, i.e., the oxygen plasma is generated in an electron cyclotron resonance (ECR) plasma source ($p_{O_2}=1.8\times10^{-3}$ mbar and plasma input power 275 W) and the oxygen ions are accelerated to the sample (the source-sample spacing is about 200 mm), which is biased by a dc voltage of −10 V during oxidation. Details of this preparation technique and the influence of the oxygen ion energy on the TMR can be found elsewhere.[6] For irradiating the oxidized Al-layer by a low energy Ar^+ ion beam (duration t_{Ion}) the ECR plasma source is operated with Ar instead of O_2 ($p_{Ar}=1.8\times10^{-3}$ mbar and plasma input power 275 W). During irradiation the sample is biased with a negative, time dependent voltage with maximum amplitude V_{Ion} [see Fig. 1(a)]. The time dependent voltage is used instead of a dc bias for avoiding arcing in the vacuum chamber at higher bias voltages. Samples with systematically varied irradiation time t_{Ion} (0–60 s) and V_{Ion} (0–430 V) are prepared. The Ar and the O ion flux densities measured by a three-grid retarding field analyzer are comparable. We have used high purity gases

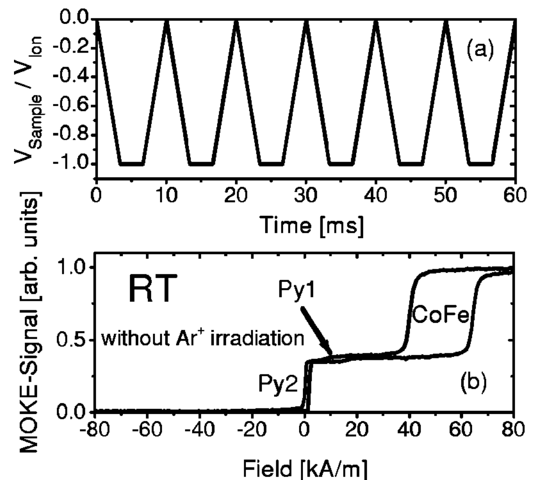

FIG. 1. (a) Schematic diagram of the time dependence of the bias voltage V_{Sample} applied to the sample during irradiating the oxidized AlO_x barrier. (b) Typical major loop of an unpatterned MTJ prepared without *in situ* ion irradiation of the barrier, measured at RT by magneto-optical Kerr effect (MOKE). The contributions of the pinned $Co_{70}Fe_{30}$ layer, the $Ni_{80}Fe_{20}$ (Py1) buffer, and the soft $Ni_{80}Fe_{20}$ (Py2) electrode to MOKE signal are labeled.

 ©2003 The American Physical Society

only (impurity level $\leqslant 0.001\%$) to avoid impurity related effects. To activate the exchange biasing of the $Co_{70}Fe_{30}$, the complete layer stack is vacuum annealed at 523 K for 5 min in a magnetic field of 80 kA/m. The stacks are then patterned by optical lithography and ion etching. Figure 1(b) shows a typical magnetization loop of a junction. The exchange bias field of the bottom $Co_{70}Fe_{30}$ electrode is about 50kA/m, which ensures well separated switching fields for the soft and the hard magnetic electrodes.

The transport measurements are performed with dc bias. The current density j (current/junction area) is measured as a function of bias voltages U, temperature T, and the external magnetic field. The area resistance product in the parallel (antiparallel) state is defined as $R_P = U/j_P$ ($R_{AP} = U/j_{AP}$), the conductance is determined correspondingly: $G_P = 1/R_P$ ($G_{AP} = 1/R_{AP}$). The mean area resistance product R is defined as $R = (R_{AP} + R_P)/2$. The amplitude of the tunneling magnetoresistance is given by $\mathrm{TMR} = (R_{AP} - R_P)/R_P$. Furthermore, we use the differential conductance in the parallel state ($G_P^{diff} = dj_P/dU$) for assessing the current-voltage characteristics of the junctions.

III. RESULTS AND DISCUSSION

A. Simulation of ion penetration depth

As discussed in the following sections, our experimental results depend essentially on the ion energy. Therefore, we start with some general remarks concerning the interaction of the ions and the sample. The Ar^+ ions penetrate into the barrier and lose their kinetic energy by inelastic electronic (ion-electron interaction) and nuclear (ion-atom collisions) energy loss. This energy transfer from the ions to the target atoms may result in a relocation (atomic mixing) and a removal (sputtering) of sample atoms. The penetration depth of the ions into the sample and, therefore, the mixing zone with relocated atoms increases with increasing ion energy.[7] Sputtering also increases with ion energy in the energy range relevant for our work.[7] For comparing the ion induced changes of the sample properties with the Ar^+ ion penetration depth we performed energy dependent Monte Carlo simulations[8] of the ion trajectories in the irradiated sample ($SiO_2/Cu^{30\,nm}/Ni_{80}Fe_{20}^{4\,nm}/Mn_{83}Ir_{17}^{15\,nm}/Co_{70}Fe_{30}^{3\,nm}/Al_2O_3^{1.8\,nm}$). The assumed barrier thickness of 1.8 nm is motivated by the often found 30% increase of the (1.4-nm-thick) metallic Al layer during oxidation[9] and agrees well with the effective barrier thickness extracted from the measured current-voltage characteristics of the reference junctions (see Sec. III C). The densities (mass/volume) of the different layers used in the simulations are taken from x-ray reflectivity measurements. Figure 2(a) shows the calculated ion fluence in the sample for different ion energies. The fluence is strongly reduced with increasing depth, whereas the penetration depth increases for higher ion energies. The energy dependence of the characteristic penetration depth d_{Ion} ("embedding depth"), defined by a reduction of the ion fluence in the sample to 2%,[9] is summarized in Fig. 2(b). For example, at 150 eV the embedding depth is equal to the assumed barrier thickness of 1.8 nm. But also for higher ion energies the penetration of the ions is still strongly localized to the barrier and the region near to the interface between the barrier and the lower electrode.

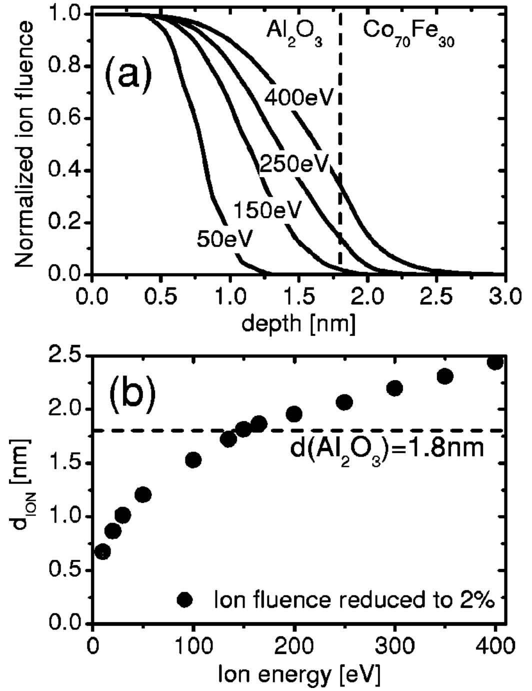

FIG. 2. (a) Normalized ion fluence in the sample for different ion energies calculated by Monte Carlo simulations. (b) Energy dependence of the characteristic ion penetration depth d_{Ion}. At d_{Ion} the ion fluence is reduced to 2%. The densities (mass/volume) of the different layers used in the simulations are taken from x-ray reflectivity measurements.

B. Magnetic properties

The magnetic properties of the soft $Ni_{80}Fe_{20}$ electrode (Py2) and the pinned $Co_{70}Fe_{30}$ layer are investigated by magneto-optical Kerr effect (MOKE). Figure 3 shows, that the coercivity H_C of the soft electrode (Py2) is not affected by the ion irradiation, indicating that the growth of the soft electrode on top of the irradiated barrier is not significantly changed. In contrast, the coupling field H_{Shift} between the ferromagnetic electrodes decreases for higher ion energy. The ferromagnetic Néel coupling field decreases exponentially with increasing thickness of the nonmagnetic spacer between the electrodes.[10] Furthermore, the Néel coupling is

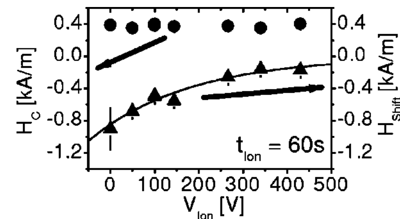

FIG. 3. Magnetic properties of the soft magnetic electrode (Py2): Coercivity H_C (●, left scale) and coupling field H_{Shift} (▲, right scale) of MTJ's with irradiated AlO_x barriers for different ion energies and fixed irradiation time, measured at RT by MOKE.

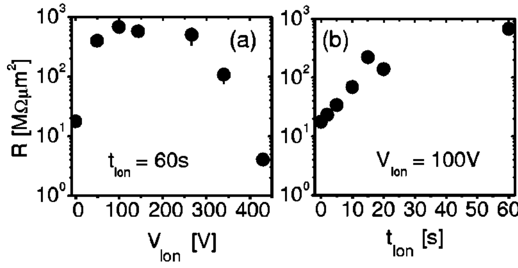

FIG. 4. Mean area resistance product R of MTJ's with irradiated AlO_x barriers for different ion energies (a) and irradiation times (b), measured at RT with a bias voltage of 10 mV.

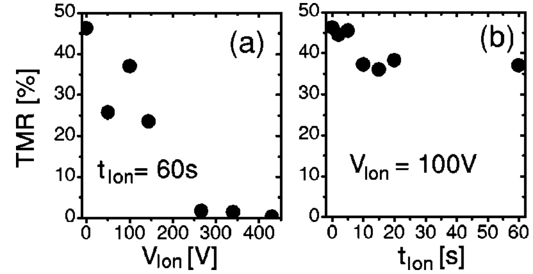

FIG. 5. Mean tunneling magnetoresistance TMR of MTJ's with irradiated AlO_x barriers for different ion energies (a) and irradiation times (b). All measurements are performed at RT with a bias voltage of 10 mV.

very sensitive to the correlation of the upper and the lower barrier interface roughness, H_{Shift} decreases for weaker correlation. Therefore, the decreasing H_{Shift} hints to a larger nonmagnetic spacer thickness after ion irradiation and a lower correlation of the interface roughness, respectively. If we include the simulated embedding depth of the Ar^+ ions (which is only larger than the Al_2O_3 thickness, if the ion energy exceeds 150 eV) for $V_{Ion} \leqslant 150$ V the reduction of the H_{Shift} hints to an increased spacer thickness, i.e., an increase of the mean atom-atom distances in the tunneling barrier. A change of the upper barrier interface roughness may also partly contribute. For higher ion energies the number of ions reaching the lower barrier interface becomes more significant and an increase of the intermixing of the tunneling barrier and the lower electrode can be expected. This further reduces the correlation of the surface roughness of both ferromagnetic electrodes and increases the thickness of the nonmagnetic spacer layer by the addition of the thin intermixing zone. Both effects reduce H_{Shift}. We like to emphasize that up to the highest ion energies the penetration of the ions into the hard magnetic electrode is limited to the first few angstroms of the Co-Fe [see Fig. 2(a)]. The interface between Co-Fe and Mn-Ir is not reached. Therefore, the strength of the exchange bias coupling energy at the FM-antiferromagnetic interface is not changed (where FM stands for ferromagnetic) and we expect only minor changes of the magnetic properties of the pinned layer. In fact, the coercivity $H_C^{Co\text{-}Fe}$ of the Co-Fe increases only slightly from 12.2 ± 1.5 kA/m to 13.9 ± 2.8 kA/m and the exchange bias field $H_{Ex}^{Co\text{-}Fe}$ of the Co-Fe becomes slightly larger. It increases from 52.2 ± 2.0 kA/m for samples without ion irradiation to 56.8 ± 2.2 kA/m for the samples irradiated at largest ion energies ($t_{Ion} = 60$ s, $V_{Ion} = 430$ V). The higher $H_{Ex}^{Co\text{-}Fe}$ after irradiation corresponds to a reduction of the nominal $Co_{70}Fe_{30}$ layer thickness by 2–3 Å, if we use the common inverse FM thickness dependence of the exchange bias.[11] This agrees with the existence of a thin intermixing zone just discussed with respect to the reduction of H_{Shift}. The influence of the ion irradiation induced structural alterations of the barrier and the barrier interface regions on the magnetotransport properties will be discussed now.

C. Area resistance product and tunneling magnetoresistance

The mean area resistance product R of MTJ's with irradiated AlO_x barriers is shown in Fig. 4. The resistance increases strongly with increasing V_{Ion} (a) up to a broad maximum between 100 V/60 s and 270 V/60 s. For V_{Ion} fixed at 100 V, the resistance increases strongly with increasing t_{Ion} [Fig. 4(b)] and hence with increasing ion dose. The changes of the barrier are, at least in the observed time scale, due to an accumulative process. Taking only direct tunneling into account this suggests that either the AlO_x becomes thicker by ion irradiation, or/and the height of the tunneling barrier increases. The mean effective barrier height and thickness[12] of the samples without ion irradiation is 2.89 ± 0.10 eV/1.76 ± 0.09 nm at RT, where an effective electron mass of $0.4 m_e$ in the barrier was assumed. Due to the exponential thickness dependence of the direct tunneling current,[12] an increase of the barrier thickness of about 3 Å can account for the resistance increase after irradiation. The increase of the barrier height (without increasing the barrier thickness) would have to be about 1.2 eV. As discussed in Sec. III D, by Cu-K_α-reflectivity measurements we have further indication that the barrier becomes thicker by ion irradiation for low ion energies. But we cannot rule out simultaneous alterations of the barrier height. The most important feature of an MTJ is its tunneling magnetoresistance (TMR). The TMR of MTJ's with irradiated AlO_x barriers is shown in Fig. 5. The TMR strongly decreases with increasing V_{Ion} (a). For ion energies higher than $V_{Ion} = 270$ V nearly no TMR is found. Simultaneously, the TMR decreases slightly for longer irradiated samples [(b) V_{Ion} fixed at 100 V].

Actually, this behavior separates most clearly the two characteristic ion energy ranges. Up to 150 V a considerable TMR is found, whereas the mean area resistance increases up to 680 M$\Omega\ \mu m^2$. For higher energy the TMR nearly vanishes and the resistance decreases. This is related to the energy dependence of the ion penetration depth. As discussed in Sec. III A the penetration of the ions is limited to the barrier for energies up to 150 eV, for higher energies the lower electrode is reached, a significant number of ions cross the lower barrier interface. In the following we discuss the influence of the ion irradiation on the structural properties of the barrier region and its possible implications for the transport properties.

For the ion energy range up to 150 V (ion penetration limited to the barrier itself) the local change of the coordination of the Al and O atoms is essential, which obviously reduces the direct tunneling conductance. Because the number of Al and O atoms is not increased during irradiation, the

experimentally indicated increase of the barrier thickness corresponds to larger mean atomic distances of Al and O in the AlO_x network. Sputtering cannot be important in this energy range, because a decrease of the barrier thickness would lead to a strong reduction of the resistance. This is compatible with the very low sputtering yield of AlO_x at low ion energy.[13] For higher energies the ion penetration is expanded to the first few angstroms of the Co-Fe and the resistance breaks down rapidly. Due to the higher energy deposition inside the barrier and the increased penetration depth of the ions atomic mixing in the barrier becomes stronger and, additionally, atomic mixing at the lower barrier interface becomes important. This can lead to an increase of the density of additional unpolarized conducting paths in the barrier, which shorten the tunneling resistance. As originally proposed by Shang *et al.*[5] to explain the temperature dependence of the magnetoresistance these conducting paths can be, e.g., chains of localized electronic states (hopping conductance) or pinholes. The formation of pinholes by the ion irradiation should be especially supposable, if the atomic mixing becomes very strong for higher ion energies. As discussed detailed in Sec. III F an increase of the conduction contribution due to defect states in the barrier after irradiation is already found for the energy range below 150 eV (ion penetration limited to the barrier itself). The further increase of this current contribution by increasing the defect density with higher ion energy is reasonable, because more energy is deposited in the barrier, which is available for defect formation. Furthermore, a reduction of the barrier thickness due to sputtering becomes more likely with higher energy. This can additionally decrease the resistance at zero bias. The increase of unpolarized current contributions reduces the TMR amplitude by shortening the spin-dependent tunneling current. But here we also have to consider alterations of the effective spin polarization of the tunneling current itself. As discussed by many authors, spin-dependent tunneling depends essentially on the atomic and electronic structure of the MTJ, i.e., particularly on the atomic positions of the barrier and electrode atoms. For example, the influence of the barrier termination on the atomic and electronic structure in $Co/Al_2O_3/Co$ junctions is pointed out by Oleinik *et al.*[14] The spin polarization can also be effected by the actual profile of the potential barrier,[15,16] the disorder in the barrier,[17] and the mechanism of bonding at the interface between the barrier and the electrode.[18] The degrading influence of nonideal interfaces on the TMR is discussed recently by Bagrets *et al.*[19] If the TMR at 4.2 K and 300 K is compared for different scattering parameters γ (see Fig. 8 in Ref. 19), a stronger relative temperature dependence TMR(300 K)/TMR(4.2 K) with increasing γ was found, that means with increasing imperfection of the interfaces between the barrier and the electrodes. Finally, magnon- and phonon-assisted tunneling can alter the TMR amplitude at room temperature[3,4] (we will come back to this in Sec. III F).

The ion irradiation changes the structure of the junction in the region near the barrier and, therefore, can imply a manifold of influences on the effective spin polarization. Starting at low ion energies (ions do not reach the lower barrier interface), the effective spin polarization may be changed, because the termination of the barrier material and the surface roughness of the upper barrier interface can be altered. Changes of the barrier potential profile like the increased thickness may also contribute. For higher ion energy (ions reach the lower barrier interface) the additional intermixing of the barrier and the bottom electrode material may be important, because the sharpness of this interface is reduced (enhanced interface imperfection). We cannot quantify the particular influence of the different possible alterations on the TMR amplitude at room temperature, but as discussed in the following sections, the changes of the dielectric stability, the investigations of the temperature, and voltage dependence of the TMR and R as well as the noise properties emphasize the importance of defect formation by the ions.

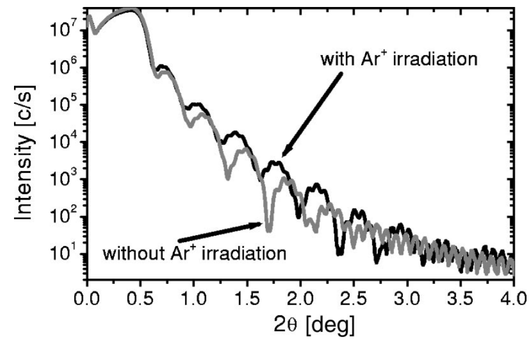

FIG. 6. Cu-K_α-reflectivity of two AlO_x multilayers: $(Al^{1.4\text{ nm}}+\text{Oxi.})_{\times 10}$ and $(Al^{1.4\text{ nm}}+\text{Oxi.}+Ar^+@[V_{Ion}=100\text{ V},t_{Ion}=60\text{ s}])_{\times 10}$, respectively.

For the application of the barrier irradiation technique, the dependence of R and TMR on the ion energy has the implication that the resistance can be adjusted over a wide range for low ion energies with good TMR amplitudes maintained at the same time. But an intentional decrease of R (which would be desirable for preparing low resistive junctions for, e.g., TMR read heads) by means of ion sputtering directly after barrier oxidation cannot be achieved.

D. Thickness of AlO_x multilayers

For measuring the barrier thickness of samples with and without ion irradiation by an independent method, we recorded the Cu-K_α-reflectivity of two specially prepared AlO_x multilayers: (a) $(Al^{1.4\text{ nm}}+\text{Oxi.})_{\times 10}$ and (b) $(Al^{1.4\text{ nm}}+\text{Oxi.}+Ar^+@[V_{Ion}=100\text{ V},t_{Ion}=60\text{ s}])_{\times 10}$, respectively. The large oscillation period in Fig. 6 corresponds to the AlO_x multilayer, the smaller period to the 100-nm-thick SiO_2 layer of the thermally oxidized Si wafer. The overall thickness d_{XRD} (where XRD stands for x-ray diffraction) of the multilayers is accurately extracted from least-squares fits[20] of these data. For sample A (without ion irradiation) we find $d_{XRD}=21.7$ nm and for sample B with ion irradiation the overall thickness is about 6% larger ($d_{XRD}=23.0$ nm). Therefore, these investigations also indicate an increase of the AlO_x thickness induced by the moderate ion irradiation. Additionally, the $\theta-2\theta$ scans of the AlO_x multilayers show no Bragg peaks which could correspond to a crystalline AlO_x phase.

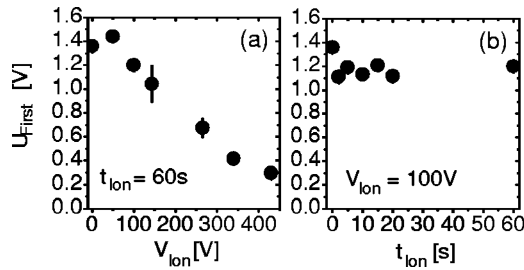

FIG. 7. Dielectric breakdown voltage U_{First} of MTJ's with irradiated AlO_x barriers for (a) different ion energies and (b) irradiation times, measured at RT.

E. Dielectric stability

An important quality for the insulating AlO_x film is its dielectric stability if high bias voltages are applied.[21] Generally, the dielectric breakdown of a tunnel junction occurs by a sudden large increase of the current at a certain applied voltage, which originates from the formation of a highly conducting localized path, shunting the tunneling resistance.[22] By voltage ramp experiments (see, e.g., Ref. 23) with a ramp speed of $dU/dt = 23$ mV s^{-1} we determined the breakdown voltage U_{First}, which denotes the voltage of the first sudden current increase. U_{First} decreases strongly with increasing V_{Ion} [Fig. 7(a), $t_{Ion} = 60$ s] to merely 300 mV at 430 V. For moderate ion energies of $V_{Ion} = 100$ V a slight reduction for longer irradiation time is found [Fig. 7(b)]. This behavior can be explained according to the E model,[24] where the breakdown process is triggered by a field induced displacement of ions in the barrier, i.e., a bond in the amorphous AlO_x network breaks up under the influence of the applied electric field. This leads to new localized states with energy levels in the band gap of the AlO_x. Charge trapping at these localized states and their wave-function overlap results in the formation of a conduction subband and a thermal run-away due to Joule heating in the final state of the breakdown process. Similar to the dielectric breakdown of thin SiO_2 films discussed by McPherson and Mogul,[24] we expect that the precursors for the bond breaks are relatively weak bonds in the amorphous AlO_x network. This may be Al-Al bonds, which result from an oxygen vacancy, or simply distorted bonds (e.g., distorted Al-O-Al). Within the framework of the E model the probability density for the breakdown process depends on one hand on the strength of the electric field, and on the other hand it is proportional to the density of the precursors. The reduction of U_{First} by ion irradiation can therefore be understood as an increase of the precursor density. This is due to the irradiation induced local change of the coordination of the Al and O atoms (see Sec. III C), which increases the mean atomic distances in the AlO_x network and obviously results in an increased number of distorted and weakened bonds. The proposed process can also be regarded as the opposite to the healing of defects in the barrier by thermal annealing, which results in a strong increase of the dielectric stability.[25] The precursor density for the dielectric breakdown increases with higher ion energy, because the penetration depth and the deposited energy increases with elevated ion energy. Furthermore, the intermixing of the barrier and the bottom electrode material at high ion energy may lead to another type of potential precursors for the dielectric breakdown at the bottom electrode-barrier interface. These additional precursors can be chemical bonds between intermixed barrier and electrode materials, respectively.

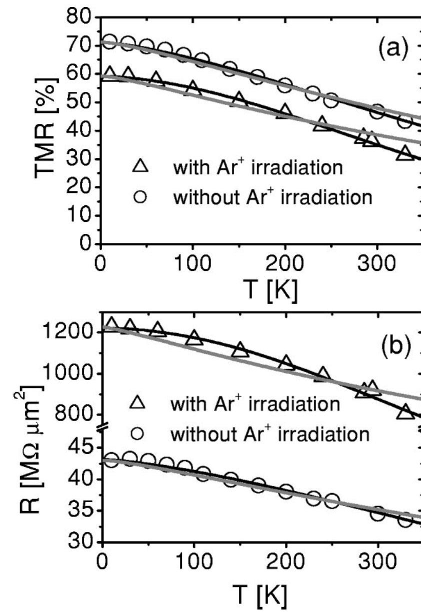

FIG. 8. Temperature dependencies of the (a) TMR and (b) the area resistance product of two MTJ's without and with irradiated AlO_x barriers ($t_{Ion} = 60$ s, $V_{Ion} = 100$ V). The black lines are fits according to Eqs. (1)–(4), the gray lines are fits according to the model of Han *et al.* (Ref. 3). All measurements are performed with a bias voltage of 10 mV.

F. Temperature and voltage dependence of the magnetoresistance

For distinguishing between different spin-polarized and unpolarized transport mechanisms in the low ion energy range, we now discuss the temperature and the voltage dependence of the magnetotransport for two junctions without ion irradiation and with softly irradiated barrier (100 V/60 s). The temperature dependence of the TMR and the area resistance product R at 10 mV bias for these samples is shown in Figs. 8(a) and 8(b). The sample without ion irradiation shows a TMR of 71.3% at 10 K, which is close to the largest reported values of Nishikawa *et al.*[26] The TMR of the irradiated sample is considerably smaller (59.3%). Both TMR and R decrease monotonically with increasing temperature. The relative temperature dependence of the area resistance product and the TMR is more pronounced for the irradiated junction. The same holds for the bias voltage dependence of the TMR [see Fig. 9(a)]. At 500 mV and 10 K (330 K) the TMR is reduced to 47% (58%) of its maximum value for the sample without irradition, whereas for the irradiated sample we find only 38% (10 K) and 37% (330 K). The conductance difference $\Delta G = G_P - G_{AP}$ depends slightly stronger on temperature for the sample without irradiation [$\Delta G(330\ \mathrm{K})/\Delta G(10\ \mathrm{K}) = 0.84$ instead of 0.87 for the irradiated sample]. Generally, the conductance can be split up

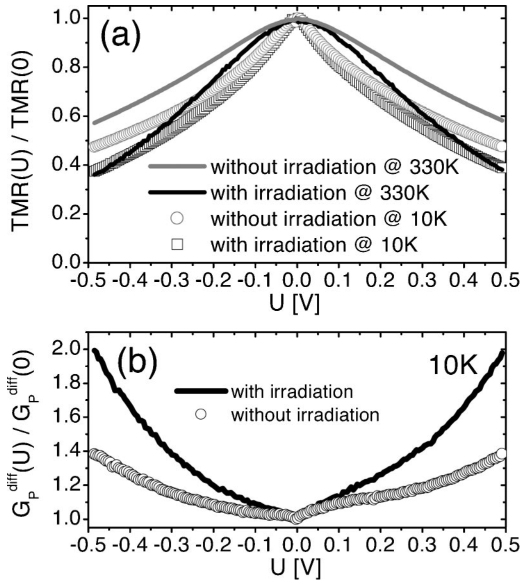

FIG. 9. Bias-voltage dependence of (a) the normalized TMR and (b) the normalized differential conductance in the parallel state $G_P^{diff} = dj_P/dU$. The irradiation is performed with $t_{Ion} = 60$ s and $V_{Ion} = 100$ V.

into a spin-polarized and an unpolarized part. The stronger bias voltage dependence of the TMR at both temperatures after irradiation implies that the voltage and temperature dependence of the unpolarized contribution is enhanced.

Different models for the temperature and the voltage dependence have been proposed up to now. First, we compare our data with models containing only a few current contributions. Han *et al.*[3] were able to fit their data of $Co_{75}Fe_{25}/AlO_x/Co_{75}Fe_{25}$ junctions by extending the model of magnon excitation developed by Zhang *et al.*[27] If we analyze the temperature [see Figs. 8(a) and 8(b)] and the voltage dependence [see Fig. 9(a)] on the basis of Eqs. (15)–(19) from this work,[28] a discrepancy between our experimental data and the proposed model is found, which is more pronounced after ion irradiation [see gray solid lines in Figs. 8(a) and 8(b)]. Especially the curvature of the theoretical curves do not accord with our temperature dependent data. This leads to the conclusion that our results cannot be explained only on the basis of magnon-assisted tunneling. In connection with this it is worth to emphasize that the TMR of our reference samples is higher than that in Ref. 3.

Dimopoulos[4] took magnon- as well as phonon-assisted tunneling into account for fitting his temperature dependent data of optimally annealed MTJ's reasonably. Magnons decrease ΔG and increase G_{AP}; phonons increase both. The addition of phonon interactions was necessary, because ΔG increased with increasing temperature, which he could only explain by an spin-conserving inelastic contribution to the tunneling current. As mentioned above, in our samples ΔG decreases with temperature, and therefore the extension of the magnon model by a phonon-assisted contribution is not unambiguously justified. Furthermore, the fit (we used a nonlinear least-squares-fitting routine based on the Levenberg-Marquardt algorithm) of our temperature dependence of G_P and G_{AP} according to Ref. 4 suffers from a high correlation of the four fitting parameters (zero-bias/zero-temperature conductance G_0, magnon contribution ΔG_{ex}, phonon contribution ΔG_{ph}, and low cutoff energy E_l of the magnons); they are therefore without a real physical meaning. The stronger temperature dependence of ΔG for the sample without ion irradiation could suggest that the phonon contribution is more important for irradiated samples. On the other hand, the stronger bias-voltage dependence of the irradiated MTJ's would imply a reduced importance of the phonon-assisted processes, in contradiction to the temperature dependence of ΔG. From this we conclude, that the extension of the magnon-assisted tunneling model by a phonon-assisted process cannot be sufficient to explain the influence of the ion irradiation on the transport properties.

The temperature dependence of MTJ's was first investigated by Shang *et al.*[5] The fit of our temperature dependent data achieved by using this phenomenological model is considerably better than the results discussed above. Shang *et al.*[5] split up the total conductance into a spin-polarized and an unpolarized contribution,

$$G(\theta,T) = G_T[1 + P_{Ni\text{-}Fe}(T) P_{Co\text{-}Fe}(T) \cos\theta] + G_{UP}(T), \tag{1}$$

where θ is the angle between the magnetization directions of the $Ni_{80}Fe_{20}$ and the $Co_{70}Fe_{30}$ electrode [therefore $G_P \equiv G(0°)$ and $G_{AP} \equiv G(180°)$]. G_T is the prefactor for direct elastic tunneling, which increases by a few percent in the investigated temperature range from 10 K to 330 K due to smearing of the Fermi distribution. We will neglect this temperature dependence in the first-order approximation and will discuss its influence below. $P_{Ni\text{-}Fe}$ and $P_{Co\text{-}Fe}$ are the effective spin polarizations of the $Ni_{80}Fe_{20}$ and the $Co_{70}Fe_{30}$ electrode, respectively. The temperature dependence of this spin polarization is assumed to be governed by spin-wave excitations[5] of the magnetization,

$$P_X(T) = P_{0,X}(1 - \alpha_X T^{3/2}) \quad \text{with} \quad X = \text{Ni-Fe, Co-Fe}, \tag{2}$$

where α_X is the spin-wave parameter and $P_{0,X}$ is the full effective spin polarization at $T = 0$ K. That means, in this model magnons influence the tunneling current via the reduction of the effective spin polarization and not by assisted tunneling processes as used in Refs. 3 and 4. In the original work by Shang *et al.*[5] the temperature dependence of the unpolarized contribution was fitted by the power law $G_{UP}(T) \propto T^\gamma$. They found a γ of 1.35 ± 0.15, which was close to the exponent 4/3 in the power-law temperature dependence of hopping through a chain of two localized states.[29] Starting from this result we assume in the following that the unpolarized conductance is dominated by hopping through localized states (which is also known to be an important transport mechanism in other amorphous barriers like Si and Ge[29]). Therefore, we write the temperature dependence of this hopping contribution at low voltage as a power series,[29]

$$G_{UP}(T) = \sum_N S_N T^{N - 2/(N+1)} \quad \text{with} \quad N = 1,2,\ldots, \tag{3}$$

TABLE I. Fit parameters determined from the temperature dependence [Eqs. (1)–(4)] of the conductance of two MTJ's without and with ion irradiation of the AlO_x barrier ($t_{Ion}=60$ s, $V_{Ion}=100$ V).

Parameter	MTJ without ion irradiation	MTJ with ion irradiation
$P_{0,Ni\text{-}Fe}\times P_{0,Co\text{-}Fe}$	0.263	0.229
G_T ($\Omega^{-1}\,\mu\text{m}^{-2}$)	$2.488\pm0.006\times10^{-8}$	$8.62\pm0.04\times10^{-10}$
$(\alpha_{Ni\text{-}Fe}+\alpha_{Co\text{-}Fe})/2$ ($K^{-3/2}$)	$1.34\pm0.04\times10^{-5}$	$1.14\pm0.06\times10^{-5}$
S_2 ($\Omega^{-1}\mu\text{m}^{-2}\text{K}^{-3/2}$)	$1.85\pm0.13\times10^{-12}$	$3.40\pm1.95\times10^{-14}$
S_2/G_T ($10^{-5}\text{K}^{-3/2}$)	7.4 ± 0.5	3.9 ± 2.3
S_3 ($\Omega^{-1}\mu\text{m}^{-2}\text{K}^{-5/2}$)	$8.74\pm1.78\times10^{-16}$	$1.53\pm0.26\times10^{-16}$
S_3/G_T ($10^{-8}\text{K}^{-5/2}$)	3.5 ± 0.7	17.7 ± 3.0

where T is the temperature in K, N is the number of participating localized states, and S_N are prefactors depending on the density of localized states in the barrier. At higher temperature the distinctive power law-temperature dependence for hopping favors chains with higher N. Another important result from Ref. 29 is the exponential thickness dependence, which also greatly favors chains in which N is large; in addition, the thickness dependence for direct tunneling is stronger than for hopping (on the other hand long chains are statistically even more rare, which limits their absolute contribution to the total conductance). Hence, an increase of the barrier thickness without changing the area density of localized states increases the relative contribution of hopping via localized states to the total conductance.

Now we apply the model of Shang *et al.*[5] to our temperature dependent data. The product $P_{0,Ni\text{-}Fe}\times P_{0,Co\text{-}Fe}$ is derived from the TMR values at 10 mV/10 K first. Then G_T and α_X are extracted from the temperature dependence of $\Delta G=G_P-G_{AP}$:

$$\Delta G\propto G_T[1-(\alpha_{Co\text{-}Fe}+\alpha_{Ni\text{-}Fe})T^{3/2}+\alpha_{CoFe}\alpha_{NiFe}T^3]. \tag{4}$$

The last term in Eq. (4) is small in the investigated temperature regime and we can neglect it. Finally, the parameters S_N are deduced from the temperature dependence of G_{AP} according to Eq. (1). The experimental data can be fitted very well [see black solid lines in Figs. 8(a) and 8(b)], if terms up to $N=3$ are taken into account. If the nonlinear least-squares fit is done with $N<3$, the χ^2 of the fit increases strongly. For $N\geqslant4$ there is no further reduction of χ^2, but the correlation between the parameters $S_{2,3,4,\ldots}$ increases strongly and these fitting parameters start to lose their physical meaning. The fitting parameters are summarized in Table I for the two samples. The product $P_{0,Ni\text{-}Fe}\times P_{0,Co\text{-}Fe}$ of the full effective spin polarizations, in fact, the general reduction of the TMR after ion irradiation, was discussed in Sec. III C with respect to structural changes at the barrier and its interfaces to the electrodes. We like to mention that the temperature independent term in Eq. (3) ($N=1$) cannot be separated from the full effective spin polarization $P_{0,X}$ at $T=0$ K. Therefore, the reduced $P_{0,X}$ can partly originate from a more pronounced unpolarized hopping conductance through one localized state, which increases both the conductance for parallel and for antiparallel alignment of the ferromagnetic electrodes. The prefactor G_T for direct elastic tunneling reflects the strongly increased area resistance product after ion irradiation, which was attributed to an increase of the effective barrier thickness in Sec. III C. The mean spin-wave parameter $(\alpha_{Ni\text{-}Fe}+\alpha_{Co\text{-}Fe})/2$ is slightly smaller after ion irradiation (due to its higher Curie temperature the contribution of Co-Fe to the mean spin-wave parameter is smaller than the contribution of Ni-Fe). This parameter is extracted from the temperature dependence of the absolute value ΔG [see Eq. (4)], which is proportional to G_T. As mentioned above, G_T increases with increasing temperature[5] (this effect is stronger for thicker and/or lower barriers), but is assumed to be temperature independent for the fitting procedure. The increase of α_X is (at least partially) due to the stronger temperature dependence of G_T, because the barrier thickness is larger after ion irradiation. The stronger decrease of the resistance for the irradiated samples with temperature is mainly reflected in a larger prefactor S_3, the ratio of this prefactor for hopping through three states and direct tunneling G_T is about five times larger for the irradiated than for the reference samples. This hints to an increase of the density of localized states in the barrier due to the ion irradiation and therefore the conductance through longer hopping chains becomes more likely. It has to be mentioned that the ratio of the prefactor S_2 for hopping through two states and direct tunneling G_T is smaller for the irradiated than for the reference samples. This seems not to be in accordance with a general increase of the hopping conductance after ion irradiation. But on the other hand, details of the spatial and energetic distribution of the localized states involved in hopping are not known and may be responsible for this inconsistency.

Finally, the increase of the hopping conductance qualitatively accords with the stronger voltage dependence of the TMR after ion irradiation [see Fig. 9(a)], which is especially more pronounced at elevated temperature. The polarized and the unpolarized conductance contribution introduced by the phenomenological model of Shang *et al.*[5] are not only temperature dependent, but both have a specific voltage dependence. As analyzed in detail by Xu *et al.*[29] the hopping conductance also increases with higher voltage, especially for larger N. Therefore, the stronger influence of the localized states on the temperature dependence suggests that the voltage dependence of the TMR should also become stronger, which is in accordance with our experimental results.

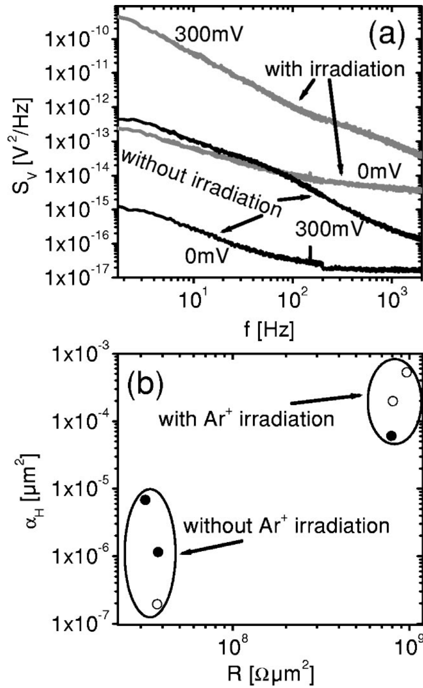

FIG. 10. (a) Power spectral density $S_V(f)$ of the noise as a function of the frequency f (measured at RT in the parallel state, bias voltages are 0 mV and 300 mV). (b) Strength of the noise, characterized by the Hooge parameter α_H, for three irradiated (100 V/60 s) and three reference samples as a function of the area resistance product R. The sample size A was 40 000 μm^2 (○) and 90 000 μm^2 (●), respectively.

For summarizing this section we can state that the temperature and the voltage dependence of the TMR and R for softly irradiated samples accords best with the phenomenological model of Shang *et al.*[5] containing unpolarized hopping conductance. The experimental data cannot be reproduced by taking only magnon excitation[3,27] or magnons and phonons[4] into account.

G. Noise properties

Because noise is a good measure for defect states in the barrier,[30] we also performed noise measurements for the irradiated and reference samples (measured at RT with 0, 10, 100, and 300 mV bias voltage in the parallel state). Figure 10(a) shows the power spectral density $S_V(f)$ of the noise measured at 0 mV and 300 mV for the two junctions discussed in the preceding section. The noise of the irradiated junction is considerable larger than the noise of the reference junction. By comparing the noise levels at 0 mV of the MTJ's with the noise of appropriate standard resistors we can conclude that these zero-bias levels are mainly due to the current input noise of the preamplifier. The low frequency noise of the MTJ can be well described by the phenomenological relation between the noise power spectral density $S_V(f)$ and frequency f, which is given by

$$S_V(f) = \alpha_H \frac{V_{dc}^2}{A f^a}. \tag{5}$$

The Hooge parameter α_H is a measure of the area normalized $1/f^a$ noise; a is the exponent which describes the slope of the frequency dependence of the noise, V_{dc} is the dc bias voltage, and A is the junction area. By fitting $S_V(f)$ at 10 Hz for different V_{dc} according to Eq. (5) we can determine α_H. Figure 10(b) shows the results for three irradiated and three reference samples. Although we have a large scatter of the data points for each set of samples, the strongly increased power spectral noise density after ion irradiation is obvious. Nowak *et al.*[30] attributed the $1/f$ noise to charge trapping processes at defect states in the barrier or near the FM-barrier interface. Trapping of an electron in a localized state would locally increase the effective barrier height, which decreases the local tunneling probability of the electrons. Therefore the higher noise after ion irradiation suggests a higher density of defect states. This is in accordance with the analysis of the temperature and the voltage dependence of the TMR, which was discussed in the preceding section and also suggested a more pronounced influence of localized states on the total conductance.

IV. CONCLUSION

In summary we have investigated the transport properties of $Mn_{83}Ir_{17}$ / $Co_{70}Fe_{30}$/AlO_x/$Ni_{80}Fe_{20}$ MTJ's whose barrier is irradiated by a low energy Ar^+ ion beam immediately after plasma oxidation. The TMR of more than 70% at 10 K/10 mV indicates the high quality of the reference junctions. The most significant effect of the additional irradiation step is an increase of the resistance up to a factor of 40 for moderate ion energy up to $V_{Ion} = 150$ V. This behavior is accompanied by a reduction of the TMR and the dielectric stability and an increase of the noise in the junctions. We conclude that this is due to an ion irradiation induced local change of the coordination of the Al and O atoms in the barrier, which leads to a thicker barrier and an increase of the precursor density for the dielectric breakdown. Furthermore, a higher contribution of the hopping conductance through localized states to the total conductance is suggested from the comparison of the measured temperature and voltage dependence of the tunneling magnetoresistance with different models. The increase of the barrier thickness is also supported by the experimental results concerning the magnetic properties and by Cu-K_α-reflectivity of AlO_x multilayers. At higher energy the resistance breaks down rapidly and the tunneling magnetoresistance vanishes completely. This results from the enhanced intermixing and sputtering of the barrier and electrode material.

ACKNOWLEDGMENTS

The authors gratefully acknowledge T. Eick for performing the noise measurements at IPHT Jena, Germany, A. Davis, T. Dimopoulos, and T. Eick for stimulating discussions; A. Thomas and M. D. Sacher for assisting the sample preparation, and S. Heitmann for assisting the XRD measurements.

*Electronic address: jschmalh@physik.uni-bielefeld.de

[1] J. Daughton, J. Appl. Phys. **81**, 3758 (1997).
[2] J.S. Moodera and G. Mathon, J. Magn. Magn. Mater. **200**, 248 (1999).
[3] X.-F. Han, A.C.C. Yu, M. Oogane, J. Murai, T. Daibou, and T. Miyazaki, Phys. Rev. B **63**, 224404 (2001).
[4] T. Dimopoulos, Ph.D. thesis, University of Strasbourg, 2002.
[5] C.H. Shang, J. Nowak, R. Jansen, and J.S. Moodera, Phys. Rev. B **58**, R2917 (1998).
[6] A. Thomas, H. Brückl, M. D. Sacher, J. Schmalhorst, and G. Reiss, J. Vac. Sci. Technol. B **21**, 2120 (2003).
[7] R. Behrisch, *Sputtering by Particle Bombardment I* (Springer-Verlag, New York, 1981).
[8] J. F. Ziegler and J. P. Biersack, *SRIM-2003. 20: The Stopping and the Range of Ions in Matter*, www.srim.org
[9] B. Roos, Ph.D. thesis, University of Kaiserslautern, 2001.
[10] J.C.S. Kools, W. Kula, D. Mauri, and T. Lin, J. Appl. Phys. **85**, 4466 (1999).
[11] J. Nogués and I.K. Schuller, J. Magn. Magn. Mater. **192**, 203 (1999).
[12] W.F. Brinkman, R.C. Dynes, and J.M. Rowell, J. Appl. Phys. **41**, 1915 (1970).
[13] Sputtering is a statistical process characterized by the sputtering yield (Y = number of removed atoms divided by the number of impinging ions). For Ar^+ ions in the energy range of some 100 eV the sputtering yield Y of AlO_x is very low [e.g., single crystalline Al_2O_3 (1102), 500 eV, normal incidence: $Y = 0.05$, Commonwealth Scientific Corp., Virginia, Bulletin No. 308]. Because the Ar-ion fluence during 60-s irradiation is comparable to the O ion fluence during 100-s oxidation, we can roughly estimate that only a few percent of the barrier atoms are removed at 500 eV. At lower energy this number is further reduced.
[14] I.I. Oleinik, E.Y. Tsymbal, and D.G. Pettifor, Phys. Rev. B **62**, 3952 (2000).
[15] S. Zhang and P.M. Levy, Eur. Phys. J. B **10**, 599 (1999).
[16] J.C. Slonczewski, Phys. Rev. B **39**, 6995 (1989).
[17] E.Y. Tsymbal and D.G. Pettifor, Phys. Rev. B **58**, 432 (1998).
[18] E.Y. Tsymbal and D.G. Pettifor, J. Phys.: Condens. Matter **9**, L411 (1997).
[19] D. Bagrets, A. Bagrets, A. Vedyayev, and B. Dieny, Phys. Rev. B **65**, 064430 (2002).
[20] Philips Electronics, WinGixa V1.102 software for Philips diffractometers.
[21] W. Oepts, H.J. Verhagen, R. Coehoorn, and W.J.M. de Jonge, J. Appl. Phys. **86**, 3863 (1999).
[22] W. Oepts, H.J. Verhagen, D.B. de Mooij, V. Zieren, R. Coehoorn, and W.J.M. de Jonge, J. Magn. Magn. Mater. **198–199**, 164 (1999).
[23] J. Schmalhorst, H. Brückl, M. Justus, A. Thomas, G. Reiss, J. Vieth, G. Gieres, and J. Wecker, J. Appl. Phys. **89**, 586 (2001).
[24] J.W. McPherson and H.C. Mogul, J. Appl. Phys. **84**, 1513 (1998).
[25] J. Schmalhorst, H. Brückl, G. Reiss, G. Gieres, and J. Wecker, J. Appl. Phys. **91**, 6617 (2002).
[26] K. Nishikawa, M. Tsunoda, S. Ogata, and M. Takahashi, IEEE Trans. Magn. **38**, 2718 (2002).
[27] S. Zhang, P.M. Levy, A.C. Marley, and S.S.P. Parkin, Phys. Rev. Lett. **79**, 3744 (1997).
[28] We assumed an equal effective spin polarization for both FM/I interfaces. The fitting procedure of the temperature dependence has only one free parameter, considerations concerning the correlation of fitting parameters are therefore not necessary.
[29] Y. Xu, D. Ephron, and M.R. Beasley, Phys. Rev. B **52**, 2843 (1995).
[30] E.R. Nowak, M.B. Weissman, and S.S.P. Parkin, Appl. Phys. Lett. **74**, 600 (1999).